HHS Public Access

Author manuscript

Cerebellum. Author manuscript; available in PMC 2019 October 01.

Published in final edited form as:

Cerebellum. 2018 October ; 17(5): 590–600. doi:10.1007/s12311-018-0951-4.

In vivo analysis of the climbing fiber – Purkinje cell circuit in SCA2-58Q transgenic mouse model

Polina A. Egorova[1], **Alexandra V. Gavrilova**[1], and **Ilya B. Bezprozvanny**[1,2,*]

[1]Laboratory of Molecular Neurodegeneration, Peter the Great St. Petersburg Polytechnic University, St. Petersburg, Russia

[2]Department of Physiology, University of Texas Southwestern Medical Center, Dallas, Texas, USA

Abstract

Cerebellar Purkinje cells (PCs) and cerebellar pathways are primarily affected in many autosomal dominant cerebellar ataxias. PCs generate complex spikes (CS) in vivo when activated by climbing fiber (CF) which rise from the inferior olive. In this study we investigated the functional state of the CF-PC circuitry in the transgenic mouse model of spinocerebellar ataxia type 2 (SCA2), a polyglutamine neurodegenerative genetic disease. In our experiments we used an extracellular single-unit recording method to compare the PC activity pattern and the CS shape in age-matched wild type mice and SCA2-58Q transgenic mice. We discovered no alterations in the CS properties of PCs in aging SCA2 mice. To examine the integrity of the olivo-cerebellar pathway we applied harmaline, an alkaloid that acts directly on the inferior olive neurons. The pharmacological stimulation of olivo-cerebellar circuit by harmaline uncovered disturbances in SCA2-58Q PC activity pattern and in the complex spike shape when compared with age-matched wild type cells. The abnormalities in the CF-PC circuitry were aggravated with age. We propose that alterations in CF-PC circuitry represent one of potential causes of ataxic symptoms in SCA2 and in other SCAs.

Keywords

Cerebellar cortex; Purkinje cells; spinocerebellar ataxias; transgenic mice; harmaline

Introduction

Spinocerebellar ataxia type 2 (SCA2) is an incurable hereditary polyglutamine neurodegenerative disease. Cerebellar Purkinje cells (PCs) are primarily affected in this disorder, atrophy of the cerebellum and brainstem is observed, also other parts of the brain involved in motor activity are affected such as the inferior olive (IO), pontocerebellar fibers, and pontine nuclei. These data were obtained by MRI visualization (1) and via *post mortem* examination of SCA2 patients (2, 3). Previous experiments on ataxia mouse models demonstrated that electrophysiological activity of aged PCs in various models of ataxia were

*Address for reprint requests and other correspondence: Dr. Ilya Bezprozvanny, 5323 Harry Hines Blvd., ND12.200, Dallas, TX 75390, USA, Ilya.Bezprozvanny@UTSouthwestern.edu.

Conflict of Interest Statement:
The authors declare that they have no conflict of interest related to this manuscript.

disturbed compared with that of PCs from age-matched wild type (WT) mice. These findings were observed in the studies with cerebellar slices from ataxia mouse models of episodic ataxia type 2 (4, 5), SCA1 (6), SCA2 (7–9), SCA3 (10), and SCA6 (11) and also with *in vivo* recordings of PC activity from anesthetized SCA2-58Q mice (12), from ataxic mice containing mutations in voltage-gated calcium channels (13, 14) and in mice expressing two different versions of CACNA1A calcium channel carboxy-terminal tail (11). However, in further experiments it was shown that neuronal dysfunction in ataxias was caused not only by PC activity dysfunction, but also by abnormalities in the climbing fiber – PC circuitry.

PC generates two types of spikes: simple spikes (SS) and complex spikes (CS). These different types of spikes are produced via two main types of afferent fibers in the cerebellum, the mossy fibers (MF) and climbing fibers (CF). MF originate from neurons in the spinal cord and brain stem and transport information from the periphery and cerebral cortex to PCs through granular cells axons forming parallel fibers (PF). CF originate in the IO nucleus and send information from the cortex to PCs by making numerous synaptic contacts with proximal dendrites of PC. CF carry excitation that makes PC generate a CS: an initial large-amplitude action potential followed by a high-frequency burst of potentials with smaller amplitude (also called spikelets). At the same time PC generates SS responding to excitatory potentials produced by PF (15–17).

Experiments conducted by Llinás and Volkind showed that harmaline administration provokes the activation of PCs via CF afferents from the inferior olive through the olivo-cerebellar system (18). Harmaline represents an alkaloid of *Peganum harmala* that induces a high frequency tremor in mammals. Llinás and Volkind also showed that harmaline acts directly on the IO neurons. They also demonstrated that harmaline-evoked PC replies have a synaptic nature (18). It was also demonstrated that systemic injections of the indole alkaloid harmaline can drive cells in the IO into higher frequency oscillations (19), thus increasing the excitatory impulse transmitted by CF to PC. Presumably, the harmaline effect on neurons of the IO is determined by attenuating voltage-sensitive calcium currents in these neurons (20). The increase of CF activity leads to the reduction of the simple spikes generation by a PC (21) due to the CF-mediated plasticity (22).

Abnormalities in the CF-PC circuitry were detected in experiments with SCA1-82Q and SCA1-30Q transgenic mice models via flavoprotein autofluorescence optical imaging and extracellular field potential recordings (23). It was demonstrated that electrical stimulation of the contralateral inferior olive (CIO) leads to the reduced response in the cerebellar cortex in transgenic mice, while responses to PF stimulation were relatively normal. Immunostaining of vesicular glutamate transporter type 2 and calbindin demonstrated a reduction in the terminals of the CF in SCA1-82Q mice (23). The disruption of the olivo-cerebellar circuit was also observed in the cell-selective mouse mutant which has a lack of functional large-conductance voltage- and calcium-activated potassium channels (BK channels) specifically in the PCs and shows a deficiency in motor coordination (24). In these mice the silencing of CS activity was observed. The rescue of CS activity in these transgenic mice was reached by harmaline intraperitoneal (IP) injections and by increasing inhibition in the deep cerebellar nuclei (DCN) via applying $GABA_A$ receptor agonists (24). However, *in*

vivo recordings of PC activity before and after IP injections of harmaline have not been previously performed in mouse models of polyglutamine-expansion disorders. In the present study the approach of pharmacological activation of the neurons in the IO was used for the evaluation of the climbing fiber – Purkinje cell circuit functional state in the SCA2-58Q transgenic mouse model.

Materials and methods

Mice breeding and genotyping

Experiments were conducted with transgenic SCA2-58Q mice and their wild type (WT) littermates. SCA2-58Q mice (25) were kindly provided to us by Dr. Stefan Pulst (University of Utah, Salt Lake City, Utah, USA) and were crossed to the FVB background. The genome of SCA2-58Q mice contains the insert of human mutant ataxin-2 protein, which has 58 CAG repeats. This transgene is driven by a L7/pcp2 promoter high specifically related to PCs (25). Mice were bred the following way: male hemizygous SCA2-58Q mice were crossed with female WT mice to generate mixed litters. The genotyping was done via PCR for *ATXN2* transgene as previously described (8, 9, 12). The volume of one PCR sample was 25 ul. The PCR mix per one sample contained: 2.5 ul 10× buffer for Taq polymerase, 0.5 ul 10mM dNTP, 1,5 ul 25mM $MgCl_2$, 0.125 ul 20 uM primers (forward and reverse), 0.25 ul Taq polymerase, 2 ul DNA, and 18 ul dH2O. The sequence of the forward primer is: 5′-GCGAACACAAAGAGAAGGACCTGGA-3′. The sequence of the reverse primer is: 5′-GCCCTTGCTTCCCGTTTTAA-3′. The PCR product has 232 bp. The animals were kept in groups of two to six in vivarium. The temperature was held 22–24°C including 12 daylight hours. The mice had access to standard food and water *ad libitum*. All procedures were approved by principles of European convention (Strasburg, 1986) and the Declaration of International medical association about humane treatment of animals (Helsinki, 1996).

Extracellular single-unit recordings *in vivo*

The method for extracellular recording of PCs activity *in vivo* was adapted from a published report (13) and was performed as previously described (12). To summarize, the mice were anesthetized with urethane with an initial concentration of 1200 mg/kg. Then in 40 minutes this concentration was increased to 1800 mg/kg. The PCs activity was recorded from 1 to 6 hours after the last injection with anesthetic. It is known, that the duration of anesthesia effect is short in case of the majority of commonly used injectable anesthetic agents such as pentobarbital or ketamine/xylazine cocktail and consists 20–40 min, while the anesthesia effect of urethane may last up to 8 hours and even more, that allowed us to perform long recording sessions. After anesthetic effects were achieved, the mice were immobilized using stereotaxic apparatus (RWD Life Science, CA). A feedback-controlled heating pad (Harvard Apparatus, MA) maintained the body temperature of the mice at 37°C. Next, the scalp under cerebellum area was taken away and a small burr hole was bored into the skull under lambdoid suture. Extracellular recordings of PCs activity were performed from IV – V cerebellar lobules using borosilicate glass pipettes (1,5 mm outer diameter, 0,86 mm inner diameter, Sutter Instruments, CA) filled with 2,5 M NaCl and resistance of 3–10 MΩ. The pipettes were advanced into the cerebellum using a one-axis oil hydraulic micromanipulator (Narishige Group, Japan) and electrical activity was continuously recorded. To establish a

baseline firing rate, neuronal pattern was observed for 5–30 min before intraperitoneal (IP) 15 mg/kg harmaline injection. The PC firing signal was identified by means of the complex spike occurrence (Fig. 1). Complex spikes are caused by climbing fiber activation that involves the generation of calcium-mediated action potentials in the dendrites, whereas simple spikes are activated synaptically by the parallel fibers otherwise known as the axons of the granule cells (17). Electrical recordings were amplified using an AC/DC Differential Amplifier (A-M Systems. Inc, WA), filtered (100 Hz high pass and 10 kHz low pass filters), digitized via analog-to-digital converter NI PCI-6221 (National Instruments, TX) and were stored for off-line computer analysis. For data acquisition and analysis, the program Bioactivity Recorder v. 5.9 was used. Statistical analysis was performed via Origin software.

According to the technique of extracellular single-unit recording in vivo the measurement of a single Purkinje cell's spike discharge is carried out with the help of a microelectrode placed in close proximity to a single neuron. Thus, the amplitude of the recording signal depends on the position of the recording microelectrode – the closer the recording microelectrode is to the cell, the higher the amplitude is. Recorded electrophysiological traces were turned upside down for off-line analysis and thus presented on the figures. It is known, that extracellular potential has opposite polarity compared to the transmembrane voltage. Indeed, we observed that recordings with lower amplitude (Fig. 2A) have opposite polarity. However, we also observed that recordings with high amplitude have the polarity of membrane potential (Fig. 2B). Since the amplitude is comparatively high in these recordings we may presume that the tip of the recording microelectrode was very close to the cell membrane, probably even forming loose-patch configuration, thus recording the membrane potential with its polarity.

Statistical analysis

During the analysis of the statistically significant differences between groups, one-way ANOVA/Bonferroni post-test were used. To analyze the electrophysiological properties of PC activity patterns, average values of simple spike frequency, complex spike frequency and post-CS pause were detected. The post-CS pause was defined as time interval from the end of CS to the first SS generation (Fig. 1). To analyze the complex spike shape, average values of complex spike duration, spikelet frequency and spikelet number were detected (Fig. 1). The obtained data on the electrophysiological phenotype of activity pattern and CS shape in WT and SCA2-58Q cerebellar PCs were presented as mean ± SE. The obtained data on the pharmacological stimulation of climbing fiber-Purkinje cell circuitry with harmaline IP injections in WT and SCA2-58Q PCs were analyzed the following way. The properties of SS and CS were calculated for three different segments of the same recording trace before injection of harmaline and for three different segments after injection of harmaline and averaged for each mouse, and then relative values were calculated for each mouse, and afterwards these relative values were averaged for each group and plotted as mean ± SE, where SE is the standard error of mean.

Results

Analysis of CS properties in SCA2-58Q mice at different ages

To analyze the functional state of the CF-PC circuitry in SCA2-58Q transgenic mice we performed a series of *in vivo* extracellular recordings of PC activity from anesthetized 6-, 9-, and 12-month-old SCA2-58Q mice and from their age-matched WT littermates. In previous experiments using in vivo recordings we demonstrated that aging PCs from SCA2-58Q mice on average generate SS with significantly higher firing frequency in comparison with WT PCs of the same age (12). However, the other properties of the activity pattern, and the features of the CS shape of aging PCs from SCA2-58Q have not been analyzed yet. To continue these experiments, we performed a series of in vivo extracellular recordings of PC activity using 6-, 9-, and 12-month-old WT mice and age-matched SCA2-58Q littermates (Figs 2A and 2B). We discovered that the rate of spontaneous complex spike firing of cerebellar PCs is reduced with age in these mice. An average rate of PC complex spike firing in WT mice was equal to 309 mHz at 6 months of age and 253 mHz at 12 months of age (Fig. 2*C*). By analyzing these data we further established that CS frequency (Fig. 2*C*) was not significantly different between WT and SCA2-58Q mice at any age ($P = 0.47$, $P = 0.13$, and $P = 0.89$ for 6-, 9-, and 12-month-old mice accordingly). We detected statistically significant difference in post-CS pause values for 9-month-old mice ($P < 0.05$, Fig. 2*D*), while for the other age groups this parameter was equal between the groups ($P = 0.12$ for 6-month-old and $P = 0.44$ for 12-month-old mice). We also did not detect any significant difference in the CS duration ($P = 0.52$, $P = 0.13$, and $P = 0.58$ for 6-, 9-, and 12-month-old mice accordingly, Fig. 2*E*) or in the spikelet frequency ($P = 0.43$, $P = 0.48$, and $P = 0.11$ for 6-, 9-, and 12-month-old mice accordingly, Fig. 2*F*) between WT and SCA2-58Q mice at any age. The number of recorded cells and the number of animals studied is given in the figure legend. Therefore, our experiments revealed that the basic properties of CS were similar in WT and SCA2-58Q mice at all ages tested.

Pharmacological stimulation of olivo-cerebellar circuit with harmaline uncovers disturbances in SCA2-58Q PC activity pattern

Next we evaluated the effect of systemic administration of harmaline. Harmaline provokes high frequency oscillations of IO neurons leading to CF-PC circuitry stimulation which forces PCs to generate complex spikes with higher firing frequency (19). In agreement with the previous studies (26, 27), in our experiments IP injections of 15 mg/kg harmaline resulted in significant increase of complex spike firing frequency and the disappearance of simple spikes from the PC discharge in both WT (Fig. 3*A, B*) and SCA2-58Q (Fig. 3*C, D*) PCs in 12 months old mice. This reciprocal firing is typical for cerebellar PCs (22, 28) and similar reciprocal response was previously observed for the electrical stimulation of the inferior olive (21, 29). With some delay, the restoration of simple spikes generation was registered as a result of harmaline washout (Fig. 3*A*, 3*B*, *right*; 3*C*, 3*D*, *right*). To quantify these data, we calculated the running average firing frequency of SS and CS in WT PC (Fig. 3*A*, *bottom*) and SCA2-58Q PC (Fig. 3*C*, *bottom*). Simple spike silent periods and following SS restoration were clearly observed in this analysis (Fig 3*A* and 3*C*).

Next, we performed quantitative analysis of CS properties after the IP injection of harmaline in 12 months old WT and SCA2-58Q mice during SS silent period (Fig. 4). We defined SS silent period as time period that lasted from the cessation of SS until their reappearance (Fig. 3*B*, *D*, *middle*). We determined that the duration of silent period was significantly longer in WT PCs when compared to SCA2-58Q PCs ($P < 0.01$, Fig. 4A). On average, this period was 660 ± 78 s for WT PCs (n = 6) and 277 ± 41 s for SCA2-58Q PCs (n = 4; $P < 0.01$). We also analyzed the CS properties during SS silent period, such as complex spike firing frequency, CS duration, and spikelet number. All these data were normalized to the same parameters of the same cell recorded before injection of harmaline. We discovered that the complex spike firing frequency in 12-month-old WT PCs increased 28.6 ± 2.4 times (n = 6) during simple spike silent period while the CS firing frequency in SCA2-58Q PCs increased only 16.4 ± 3.6 times (n = 4; $P < 0.05$) (Fig 4B). We also found out that the average CS duration for WT mice was decreased by 33 ± 6% (n = 6) but it was increased by 29 ± 11% (n = 4; $P < 0.01$) for the age-matched SCA2-58Q mice during SS silent period (Fig 4C). We detected that the average spikelet number for WT mice was decreased by 22 ± 5% (n = 6) but it was increased by 11 ± 13% (n = 4; $P < 0.05$) for the age-matched SCA2-58Q mice during SS silent period (Fig. 4D). These results suggested that injection of harmaline resulted in opposite changes in PC cell firing in 12 months old WT mice and in age-matched SCA2-58Q mice.

Progressive abnormalities in the climbing fiber – Purkinje cell circuitry are observed in aging SCA2-58Q mice

To analyze the age-dependent changes in the olivo-cerebellar circuit, we continued *in vivo* extracellular recordings of PC activity after IP injections of harmaline in anesthetized SCA2-58Q mice and their WT littermates at the age of 9 months (Fig 5*A*) and 12 months (Fig 5*B*). In contrast to 12-month-old mice, much less PC cells with simple spike silent periods were observed in response to harmaline injections in the 9-month-old WT or SCA2-58Q mice (3 PCs out of 13). To quantify these data, we determined the properties of SS and CS before injection of harmaline and 40 min after injection of harmaline in each group of mice (average of 3 segments for each time point). The values measured at 40 min time point were normalized to the same parameters of the same cell recorded before injection of harmaline. In this analysis we determined that 40 min after harmaline administration the frequency of CS generation was increased 54.2 ± 13.7 times (n = 6 cells) in 9-month-old WT PCs and 17.9 ± 6.0 times (n = 7 cells; $P < 0.05$) in SCA2-58Q PCs of the same age (Fig 5C). In 12-month-old WT PCs the complex spike frequency was increased 25.6 ± 2.8 times (n = 6 cells), while in 12-month-old SCA2-58Q PCs it was increased only 8.9 ± 4.0 times (n = 5; $P < 0.01$, Fig. 5*C*). Injection of harmaline caused similar reduction in SS firing frequency in 9 months old WT and SCA2-58Q mice ($P = 0.69$, Fig 5D). In contrast, in 12 months old mice injection of harmaline resulted in 93.4 ± 4.1% (n = 6) decrease in the simple spike firing frequency in WT mice and 62.2 ± 13.2% (n = 5; $P < 0.05$, Fig 5D) reduction in SCA2-58Q mice. We also observed the significant difference in relative post-CS pause between 9 months old WT and SCA2-58Q mice. Thus, the post-CS pause was increased 5.3 ± 1.4 times (n = 6) in 9-month-old WT PCs and 2.12 ± 0.2 times (n = 7 cells; $P < 0.05$, Fig. 5*E*) in SCA2-58Q PCs of the same age. In contrast, no significant

difference was observed in relative post-CS pause between 12 months old WT and SCA2-58Q mice ($P = 0.38$, Fig. 5*E*).

In addition, we analyzed the effect of harmaline IP injection on the CS shape of PCs from 9 months and 12 months old SCA2-58Q and WT mice (Fig. 6). No significant differences between relative complex spike duration, relative spikelet frequency, and relative spikelet number were observed for 9-month-old WT and SCA2-58Q PCs after harmaline IP injection ($P = 0.13$, $P = 0.15$, and $P = 0.39$ accordingly; Fig. 6). In contrast, in 12 months old mice injection of harmaline resulted in 34.5 ± 5.9% (n = 6) decrease in the complex spike duration in WT mice and 21.2 ± 15.92% (n = 5; $P < 0.01$, Fig 6) increase in SCA2-58Q mice. No significant difference between relative spikelet frequencies was observed for 12-month-old WT and SCA2-58Q PCs after harmaline IP injection ($P = 0.45$, Fig. 6). In 12-month-old WT PCs the spikelet number was decreased 23.9 ± 4.5% (n = 6 cells), while in 12-month-old SCA2-58Q PCs it was increased 12.0 ± 8.7% (n = 5 cells; $P < 0.01$, Fig. 6).

Obtained results suggested progressive disturbances of PC activity pattern and CS shape in aging SCA2-58Q PCs which were revealed by pharmacological stimulation of climbing fiber – Purkinje cell circuitry with harmaline.

Discussion

Purkinje cells generate simple spikes when activated mostly by the pontocerebellar system, but also by other pathways including vestibular nerve and nuclei, the spinal cord, the reticular formation, and feedback from deep cerebellar nuclei (30). The complex spikes are generated by Purkinje cells in response to an excitation coming by way of the olivocerebellar pathway (16). The inferior olive is the exclusive source of climbing fibers to the cerebellum. An axon from each olivary neuron terminates in multiple synapses on the proximal dendrites of Purkinje cells. When a climbing fiber discharges, it evokes climbing fiber responses (called complex spikes) in Purkinje cells (19). The complex spike waveform is highly variable. The duration of complex spike, the number and frequency of spikelets are varying from cell to cell. This diversity suggests that CS shape could be a significant characteristic of olivocerebellar activity. The origin of this variability is not well known (31). Interestingly, there is a suggestion that vestibular stimulus lead to the oscillations in complex spikes, and that might provide a mechanism by which the vestibule-olivo-cerebellum contributes to adaptation to periodic motion (19). In this study we decided to perform recordings from anesthetized animals, without any motor activity, to exclude the possibility of climber fiber activation in reply to physical stimulants that may affect the vestibular system, visuomotor control, and other sources. However, in the future we plan to expand these experiments to awake animals.

In previous experiments via extracellular recording in vivo we demonstrated that aging PCs from SCA2-58Q mice on average fire more frequently and less regularly than age-matched PCs from WT mice (12). In the present study we observed the difference in response to harmaline between aging SCA2-58Q and WT PCs. At 9 months of age the increase in CS firing frequency was detected for both mouse lines (Fig. 5*C*), but only few PCs with SS silent periods were observed. At 12 months of age injection of harmaline induced SS silent

periods in both SCA2 and WT mice (Fig. 3), but in SCA2 mice the mean duration of SS silent periods was less than in WT mice (Fig 4A). The observation of SS silent periods may be explained by the fact that the climbing fiber stimulation disrupts PC activity (21, 29). It is well known that there are at least two forms of CF-mediated plasticity (22). The CF activation leads to the potentiation of the synapses between the PF and molecular layer interneuron and between the molecular layer interneuron and PC. The simultaneous depression of the synapse between the PF and PC is observed (22) that explains the abolishment of SS in PC discharge after harmaline injection. The shorter SS silent periods or their absence in 12-month-old SCA2-58Q PCs can be explained by the fact that during the wash out period the lower harmaline concentration still causes SS inhibition in WT PCs in comparison with SCA2-58Q PCs of the same age, that may be explained by the reduced CF translocation that was observed previously in SCA1-82Q transgenic mice (23). Presumably, the SS silent periods are observed in 12-month-old PCs, but not in younger mice, because of the age-related changes in CF-mediated plasticity in these mice. During SS silent period in 12 months old mice CS frequency was increased in both WT and SCA2-58Q mice, but increase in WT mice was more dramatic (Fig 4B). During SS silent periods in 12-month-old mice the injection with harmaline led to the shortening of the CS duration (Fig. 4C) and the decrease in spikelet number in WT mice (Fig. 4D), while these parameters were increased in SCA2-58Q mice of the same age.

We also performed the analysis of data recorded 40 min after harmaline injection. At 9 months of age the significant difference between the relative CS firing frequency (Fig. 5*C*) and relative post-CS pause (Fig. 5*E*) in SCA2-58Q and WT mice was detected, but relative SS firing frequency was similar (Fig. 5*D*). At 12 months of age significant difference in the relative CS frequency (Fig. 5*C*) and relative SS frequency (Fig. 5*D*) was detected between WT and SCA2-58Q mice 40 min after injection of harmaline. The increase in CS frequency (Fig 5*C*) and post-CS pause (Fig. 5*E*) was abated in SCA2 mice when compared to WT mice. At 12 months of age, the reduction in SS firing frequency was less dramatic in SCA2 mice when compared to WT mice (Fig. 5*D*). Experimental evidences demonstrated that spikelets of the complex spikes are formed by dendritic calcium currents (32, 33), but in recent studies on parasagittal cerebellar slices via whole-cell patch-clamp recordings it was shown that dendritic spikes are not necessary for the generation of the complex spike (16). After a complex spike occurrence the post-CS pause is observed. The mechanisms underlying the generation and duration of this pause are not well understood. It was previously shown that the post-CS pause length depends on the spontaneous simple spike firing rate (34). Recently it was shown that the duration of the pause also strongly depends on the number of dendritic calcium spikes triggered by climbing fiber input and that might occur through the activation of calcium-activated potassium channels (16). Thus, longer duration of the post-complex spike pause is observed when there are more climbing fiber discharges coming to Purkinje cell. This is consistent with our finding that the relative post-complex spike pause in 9 months old WT PCs enhanced more than in SCA2-58Q PCs of the same age after harmaline injection (Fig. 5*E*).

In our experiments after IP injection of harmaline the reduction of the complex spike duration in WT PCs was observed, while the CS duration in SCA2-58Q PCs was increased (Fig. 4*C*, Fig. 6). It is well known that harmaline drives neurons in the inferior olive into

higher frequency oscillations (19) and we assume that these oscillations lead to shorter bursts in climbing fibers that explains the reduction in complex spike duration in WT PCs after harmaline injection. This assumption might also explain the observed reduction in the spikelet number in WT PCs with their increase in SCA2-58Q PCs after harmaline injection (Fig. 3*D*, Fig. 6). We suggest that the increase in CS duration and spikelet number after harmaline injection in SCA2-58Q PCs might be explained by the disruption of the CF-PC synapse in these transgenic mice that may provoke longer bursts in their CF terminals.

Thus, our findings revealed the progressive dysfunction of the climbing fiber – Purkinje cell circuitry in aging SCA2-58Q mice. In our study SCA2-58Q transgenic mice were used. Their genome contains the insert of human mutant Atxn2 protein, which has 58 CAG repeats. The expression of the Atxn2 transgene is PC-specific in these mice due to the PC-specific L7/pcp2 promoter (25). Thus, we may conclude that the observed olivocerebellar tract defects develop initially in postsynaptic PCs. The evidence suggests that regular PC physiology is required for normal CF morphology and function (23). In our previous experiments via extracellular recordings *in vivo* it was shown that the electrophysiological activity of PCs is altered in aging SCA2-58Q mice (12) and, therefore, may affect the functional state of CF and CF-PC circuitry. Dysfunction of SCA2-58Q PCs may cause the loss of synaptic connections between PC dendrites and CF terminals that may lead to the impaired LTD in SCA2 mice. The observation of SS silent periods after systemic administration of harmaline in 12-month-old mice might be explained by the CF-mediated LTD and shorter SS silent periods in SCA2 mice might be caused by the disturbed LTD in these mice.

There is also a possibility of developmental causes that may lead to the alterations in the PC reply to the harmaline-mediated climbing fiber activation in SCA2-58Q mice. It was previously shown that the disruption in the olivocerebellar circuitry leads to severe motor deficits (22). The abnormalities in the climbing fiber development have been observed in mouse models of SCA1, SCA7, SCA14, and SCA23. These impairments vary from the disturbances in climbing fiber formation during ontogenetic development to CF reduction in the cerebellum from adult mice (35). In our case we cannot exclude the possibility of a developmental component, but basic properties of complex spikes were similar in SCA2-58Q and WT mice at different ages (Fig. 2) and only at 12 months of age we observed statistically significant difference in the CS shape of SCA2-58Q PCs in response to the harmaline administration (Fig. 6). From these results we concluded that developmental causes have mild effect on the CF-PC circuitry in SCA2-58Q aging mice. There is evidence that in SCAs the neuronal calcium signaling is altered (36–38). Thus, the disturbed calcium signaling in PC cells may also contribute to the alterations of the CF-PC circuitry in SCA2-58Q transgenic mice.

Our study showed that the properties of the complex spikes were not significantly different in aging WT and SCA2-58Q mice. We also demonstrated significant difference in PC responses to systemic administration of harmaline in aging WT and SCA2-58Q mice. We propose that changes in responses to the olivo-cerebellar pathway stimulation might be explained by the alterations in the climbing fiber – Purkinje cell circuitry in SCA2-58Q transgenic mice. Climbing fiber input to the cerebellum is thought to instruct associative

motor memory formation through its effects on multiple sites within the cerebellar circuit (39). Thus, the impairment of motor coordination in aging SCA2-58Q mice might be caused by the alterations in PC activity such as simple spike generation (12), but also by the disturbances in olivo-cerebellar pathway since the stimulation of this pathway leads to different response in aging WT and SCA2-58Q mice (Fig. 3–6).

CF represents one of the major excitatory PC inputs and CF-mediated cerebellar plasticity is crucial for normal cerebellar functioning (30). The disruption of the synapse between CF and PC may be a common feature among the SCAs (35). It is becoming evident that early symptoms of ataxia may result not from PC death but from PC dysfunction and loss of firing precision (7–10, 12, 40). The malfunction of CF-PC circuitry that we observed in SCA2-58Q transgenic mice might impair the information transfer within olivo-cerebellar circuit that could contribute to the disturbance of motor functions detected in these mice, eventually leading to ataxic phenotype. However, more functional studies are required to test the hypothesis concerning the alterations in CF-PC synapse as a common pathology among the SCAs, and a possibility of using this synapse as a therapeutic target.

Conclusion

The climbing fiber originates in the inferior olive and extends to the Purkinje cell proximal dendrites. Climbing fiber input triggers the complex spike generation by Purkinje cell. Using extracellular single-unit recordings we established that functional state of climbing fiber – Purkinje cell circuitry is impaired in aging SCA2-58Q mice. The impairment was more dramatic in 12 months old mice than in 9 months old mice. We propose that alterations in CF-PC circuitry represent one of potential causes of ataxic symptoms in SCA2 and possibly other SCAs.

Acknowledgments

We are grateful to members of Laboratory of Molecular Neurodegeneration for advice and suggestions and to Polina Plotnikova for administrative assistance. IB is a holder of the Carl J. and Hortense M. Thomsen Chair in Alzheimer's Disease Research. PE is a holder of Presidential Stipend 3635.2016.4. This work was supported by the National Institutes of Health R01NS056224 (IB), by the state grant 17.991.2017/4.6 (IB) and by the Russian Science Foundation Grant 14-25-00024-П (IB). The financial support was divided in the following way: experiments depicted on Figure 1 and 2 were supported by the state grant 17.991.2017/4.6, experiments depicted on Figure 3, 4, 5 and 6 were supported by the Russian Science Foundation Grant 14-25-00024-П.

References

1. Burk K, Abele M, Fetter M, Dichgans J, Skalej M, Laccone F, et al. Autosomal dominant cerebellar ataxia type I clinical features and MRI in families with SCA1, SCA2 and SCA3. Brain. 1996; 119(Pt 5):1497–505. [PubMed: 8931575]
2. Geschwind DH, Perlman S, Figueroa CP, Treiman LJ, Pulst SM. The prevalence and wide clinical spectrum of the spinocerebellar ataxia type 2 trinucleotide repeat in patients with autosomal dominant cerebellar ataxia. American journal of human genetics. 1997; 60(4):842–50. [PubMed: 9106530]
3. Lastres-Becker I, Rub U, Auburger G. Spinocerebellar ataxia 2 (SCA2). Cerebellum. 2008; 7(2): 115–24. [PubMed: 18418684]
4. Alvina K, Khodakhah K. The therapeutic mode of action of 4-aminopyridine in cerebellar ataxia. J Neurosci. 2010; 30(21):7258–68. [PubMed: 20505092]

5. Walter JT, Alvina K, Womack MD, Chevez C, Khodakhah K. Decreases in the precision of Purkinje cell pacemaking cause cerebellar dysfunction and ataxia. Nat Neurosci. 2006; 9(3):389–97. [PubMed: 16474392]
6. Dell'Orco JM, Wasserman AH, Chopra R, Ingram MA, Hu YS, Singh V, et al. Neuronal Atrophy Early in Degenerative Ataxia Is a Compensatory Mechanism to Regulate Membrane Excitability. J Neurosci. 2015; 35(32):11292–307. [PubMed: 26269637]
7. Hansen ST, Meera P, Otis TS, Pulst SM. Changes in Purkinje cell firing and gene expression precede behavioral pathology in a mouse model of SCA2. Hum Mol Genet. 2013; 22(2):271–83. [PubMed: 23087021]
8. Kasumu AW, Liang X, Egorova P, Vorontsova D, Bezprozvanny I. Chronic suppression of inositol 1,4,5-triphosphate receptor-mediated calcium signaling in cerebellar purkinje cells alleviates pathological phenotype in spinocerebellar ataxia 2 mice. J Neurosci. 2012; 32(37):12786–96. [PubMed: 22973002]
9. Kasumu AW, Hougaard C, Rode F, Jacobsen TA, Sabatier JM, Eriksen BL, et al. Selective positive modulator of calcium-activated potassium channels exerts beneficial effects in a mouse model of spinocerebellar ataxia type 2. Chemistry & biology. 2012; 19(10):1340–53. [PubMed: 23102227]
10. Shakkottai VG, do Carmo Costa M, Dell'Orco JM, Sankaranarayanan A, Wulff H, Paulson HL. Early changes in cerebellar physiology accompany motor dysfunction in the polyglutamine disease spinocerebellar ataxia type 3. J Neurosci. 2011; 31(36):13002–14. [PubMed: 21900579]
11. Mark MD, Krause M, Boele HJ, Kruse W, Pollok S, Kuner T, et al. Spinocerebellar ataxia type 6 protein aggregates cause deficits in motor learning and cerebellar plasticity. J Neurosci. 2015; 35(23):8882–95. [PubMed: 26063920]
12. Egorova PA, Zakharova OA, Vlasova OL, Bezprozvanny IB. In vivo analysis of cerebellar Purkinje cell activity in SCA2 transgenic mouse model. Journal of neurophysiology. 2016; 115(6):2840–51. [PubMed: 26984424]
13. Gao Z, Todorov B, Barrett CF, van Dorp S, Ferrari MD, van den Maagdenberg AM, et al. Cerebellar ataxia by enhanced Ca(V)2.1 currents is alleviated by Ca2+-dependent K+-channel activators in Cacna1a(S218L) mutant mice. J Neurosci. 2012; 32(44):15533–46. [PubMed: 23115190]
14. Hoebeek FE, Stahl JS, van Alphen AM, Schonewille M, Luo C, Rutteman M, et al. Increased noise level of purkinje cell activities minimizes impact of their modulation during sensorimotor control. Neuron. 2005; 45(6):953–65. [PubMed: 15797555]
15. Burroughs A, Wise AK, Xiao J, Houghton C, Tang T, Suh CY, et al. The dynamic relationship between cerebellar Purkinje cell simple spikes and the spikelet number of complex spikes. J Physiol. 2017; 595(1):283–99. [PubMed: 27265808]
16. Davie JT, Clark BA, Hausser M. The origin of the complex spike in cerebellar Purkinje cells. J Neurosci. 2008; 28(30):7599–609. [PubMed: 18650337]
17. Raman IM, Bean BP. Ionic currents underlying spontaneous action potentials in isolated cerebellar Purkinje neurons. J Neurosci. 1999; 19(5):1663–74. [PubMed: 10024353]
18. Llinas R, Volkind RA. The olivo-cerebellar system: functional properties as revealed by harmaline-induced tremor. Exp Brain Res. 1973; 18(1):69–87. [PubMed: 4746753]
19. Barmack NH. Inferior olive and oculomotor system. Progress in brain research. 2006; 151:269–91. [PubMed: 16221592]
20. Zhan X, Graf WM. Harmaline attenuates voltage--sensitive Ca(2+) currents in neurons of the inferior olive. Journal of pharmacy & pharmaceutical sciences: a publication of the Canadian Society for Pharmaceutical Sciences, Societe canadienne des sciences pharmaceutiques. 2012; 15(5):657–68.
21. Zucca R, Rasmussen A, Bengtsson F. Climbing Fiber Regulation of Spontaneous Purkinje Cell Activity and Cerebellum-Dependent Blink Responses(1,2,3). eNeuro. 2016; 3(1)
22. Badura A, Schonewille M, Voges K, Galliano E, Renier N, Gao Z, et al. Climbing fiber input shapes reciprocity of Purkinje cell firing. Neuron. 2013; 78(4):700–13. [PubMed: 23643935]
23. Barnes JA, Ebner BA, Duvick LA, Gao W, Chen G, Orr HT, et al. Abnormalities in the climbing fiber-Purkinje cell circuitry contribute to neuronal dysfunction in ATXN1[82Q] mice. J Neurosci. 2011; 31(36):12778–89. [PubMed: 21900557]

24. Chen X, Kovalchuk Y, Adelsberger H, Henning HA, Sausbier M, Wietzorrek G, et al. Disruption of the olivo-cerebellar circuit by Purkinje neuron-specific ablation of BK channels. Proc Natl Acad Sci U S A. 2010; 107(27):12323–8. [PubMed: 20566869]
25. Huynh DP, Figueroa K, Hoang N, Pulst SM. Nuclear localization or inclusion body formation of ataxin-2 are not necessary for SCA2 pathogenesis in mouse or human. Nat Genet. 2000; 26(1):44–50. [PubMed: 10973246]
26. Karelina TV. Effect of harmaline on firing pattern of rat cerebellar Purkinje cells in ontogenesis. Zhurnal evoliutsionnoi biokhimii i fiziologii. 2008; 44(1):78–82. [PubMed: 18411517]
27. Stratton SE, Lorden JF, Mays LE, Oltmans GA. Spontaneous and harmaline-stimulated Purkinje cell activity in rats with a genetic movement disorder. J Neurosci. 1988; 8(9):3327–36. [PubMed: 3171680]
28. Jin XH, Wang HW, Zhang XY, Chu CP, Jin YZ, Cui SB, et al. Mechanisms of Spontaneous Climbing Fiber Discharge-Evoked Pauses and Output Modulation of Cerebellar Purkinje Cell in Mice. Frontiers in cellular neuroscience. 2017; 11:247. [PubMed: 28878623]
29. Demer JL, Echelman DA, Robinson DA. Effects of electrical stimulation and reversible lesions of the olivocerebellar pathway on Purkinje cell activity in the flocculus of the cat. Brain research. 1985; 346(1):22–31. [PubMed: 3876867]
30. Ito M. The modifiable neuronal network of the cerebellum. Jpn J Physiol. 1984; 34(5):781–92. [PubMed: 6099855]
31. Lang EJ, Tang T, Suh CY, Xiao J, Kotsurovskyy Y, Blenkinsop TA, et al. Modulation of Purkinje cell complex spike waveform by synchrony levels in the olivocerebellar system. Frontiers in systems neuroscience. 2014; 8:210. [PubMed: 25400556]
32. Eccles JC, Llinas R, Sasaki K. The excitatory synaptic action of climbing fibres on the Purkinje cells of the cerebellum. J Physiol. 1966; 182(2):268–96. [PubMed: 5944665]
33. Campbell NC, Hesslow G. The secondary spikes of climbing fibre responses recorded from Purkinje cell somata in cat cerebellum. J Physiol. 1986; 377:207–24. [PubMed: 3795087]
34. Armstrong DM, Rawson JA. Activity patterns of cerebellar cortical neurones and climbing fibre afferents in the awake cat. J Physiol. 1979; 289:425–48. [PubMed: 458677]
35. Smeets CJ, Verbeek DS. Climbing fibers in spinocerebellar ataxia: A mechanism for the loss of motor control. Neurobiology of disease. 2016; 88:96–106. [PubMed: 26792399]
36. Egorova P, Popugaeva E, Bezprozvanny I. Disturbed calcium signaling in spinocerebellar ataxias and Alzheimer's disease. Seminars in cell & developmental biology. 2015; 40:127–33. [PubMed: 25846864]
37. Matilla-Duenas A, Ashizawa T, Brice A, Magri S, McFarland KN, Pandolfo M, et al. Consensus paper: pathological mechanisms underlying neurodegeneration in spinocerebellar ataxias. Cerebellum. 2014; 13(2):269–302. [PubMed: 24307138]
38. Egorova PA, Bezprozvanny IB. Inositol 1,4,5-trisphosphate receptors and neurodegenerative disorders. The FEBS journal. 2017
39. Mathews PJ, Lee KH, Peng Z, Houser CR, Otis TS. Effects of climbing fiber driven inhibition on Purkinje neuron spiking. J Neurosci. 2012; 32(50):17988–97. [PubMed: 23238715]
40. De Zeeuw CI, Hoebeek FE, Bosman LW, Schonewille M, Witter L, Koekkoek SK. Spatiotemporal firing patterns in the cerebellum. Nature reviews Neuroscience. 2011; 12(6):327–44. [PubMed: 21544091]

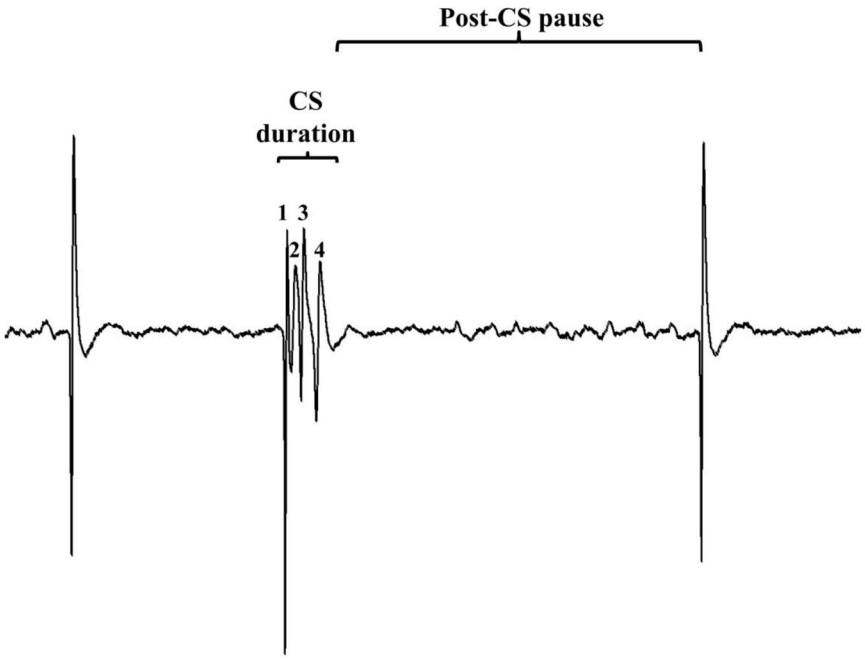

Figure 1. The properties of complex spike

Complex spike (CS) duration and post-CS pause are shown on the figure. Spikelets of the CS are indicated by numbers from 1 to 4, thus number of spikelets here, n = 4. The spikelet frequency is the number of spikelets per the CS duration.

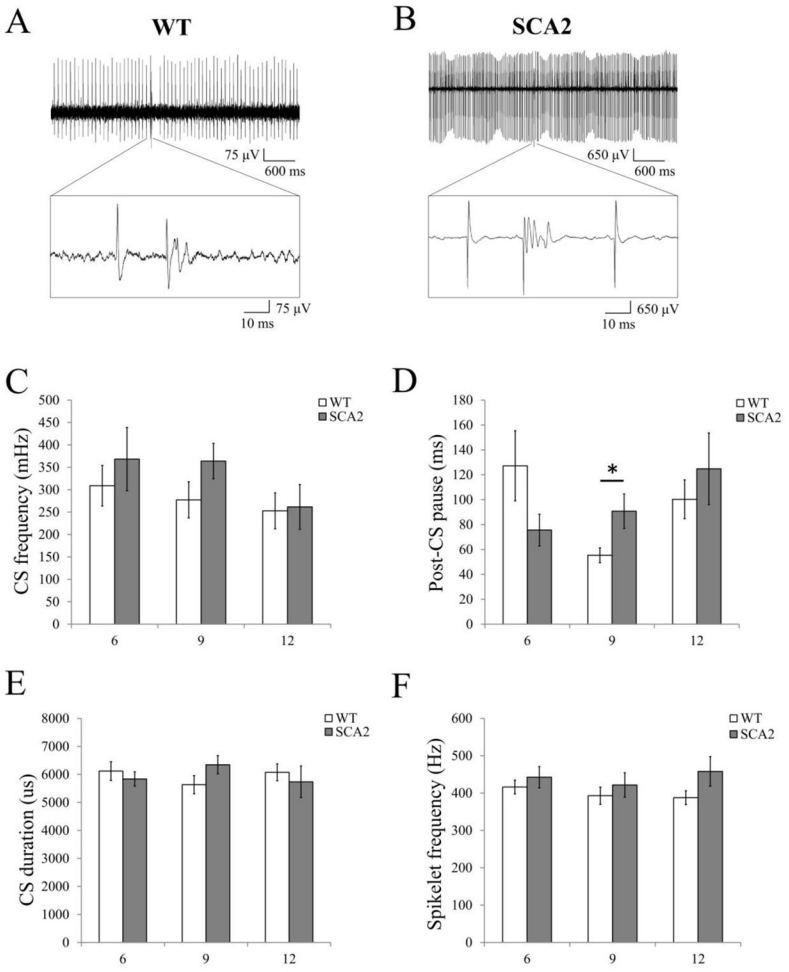

Figure 2. In vivo recordings of complex spikes generated by Purkinje cells in wild type and SCA2-58Q mice at different ages

(A, B) Examples of PC firing activity in 12 month old WT (A) and SCA2-58Q (B) mice. Recording traces are 5 s in duration with enlarged 100-ms fragment containing CS is shown.

(C) The average CS firing frequency of PCs for 6-, 9- and 12-month-old WT (n = 33, 32 and 32 cells; m = 15, 10 and 12 mice) and SCA2-58Q mice (n = 27, 34 and 26 cells; m = 10, 13 and 14 mice) are shown as mean ± SE. No statistically significant difference was observed.

(D) The average post-CS pause in PCs discharge for 6-, 9- and 12-month-old WT (n = 32, 30 and 31 cells; m = 15, 10 and 12 mice) and SCA2-58Q mice (n = 26, 25 and 26 cells; m = 10, 13 and 14 mice) are shown as mean ± SE. $*P < 0.05$.

(E, F) The average CS duration (*E*) and spikelet number (*F*) for WT and SCA2-58Q mice at 6 months of age (m = 15 and 10 mice), 9 months of age (m = 10 and 13 mice), and 12 months of age (m = 12 and 14 mice) are shown as mean ± SE. No statistically significant difference was observed.

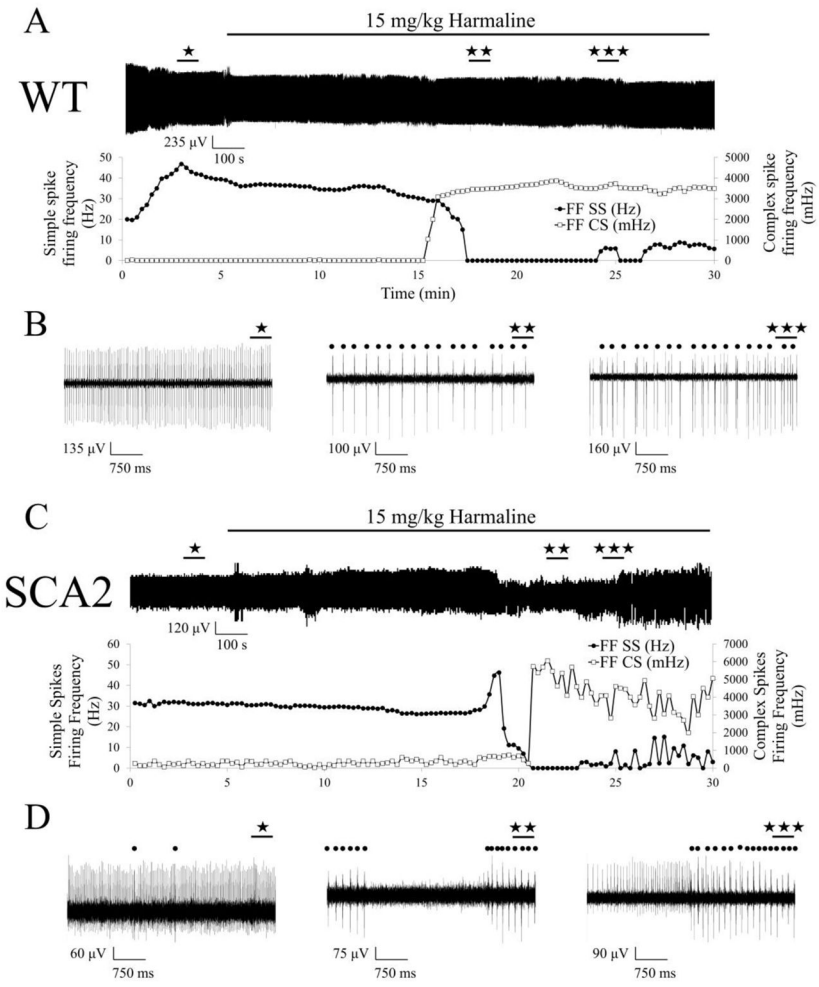

Figure 3. Changes in activity of Purkinje cells induced by injection of harmaline in 12 months old wild type and SCA2-58Q mice

(A) Continuous 30-min recording of PC activity from 12-month-old WT mouse. The time of the 15 mg/kg harmaline IP injection is indicated by a horizontal bar above the recording. Plots of the running average of simple spike firing frequency (filled circles -●-) and of the running average of complex spike firing frequency (open squares -□-) are shown below the recording.

(B) 5-s fragments of WT PC activity recordings before injection of harmaline (★), after injection during simple spikes silent period (★★) and after simple spike restoration (★★★) are shown on the expanded timescale. Complex spikes are marked by filled circles.

(C) Continuous 30-min recording of PC activity from 12-month-old SCA2 mouse. The time of 15 mg/kg harmaline IP injection is indicated by a horizontal bar above the recording. Plots of the running average of simple spike firing frequency (filled circles -●-) and of the running average of complex spike firing frequency (open squares -□-) are shown below the recording.

(D) 5-s fragments of SCA2-58Q PC activity recordings before injection of harmaline (★), after injection during simple spikes silent period (★★) and after simple spike restoration (★★★) are shown on the expanded timescale. Complex spikes are marked by filled circles.

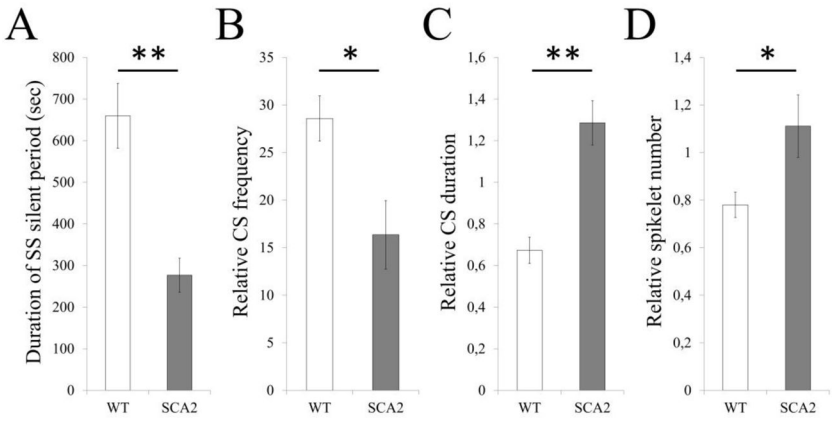

Figure 4. Analysis of changes in activity of Pukinje cells resulting from injections of harmaline in 12 months old wild type and SCA2-58Q mice

(A) The average duration of simple spike silent periods in PCs discharge is shown for 12 months old WT (n = 6 cells; m = 6 mice) and SCA2-58Q mice (n = 4 cells; m = 4 mice). Data are means ± SE. $^{**}P < 0.01$.

(B–D) Relative changes in CS firing frequency (B), CS duration (C), and spikelet number (D) during silent period are shown for 12 months old WT (n = 6 cells; m = 6 mice) and SCA2-58Q mice (n = 4 cells; m = 4 mice). For each cell the values were normalized to the same parameters of the same cell recorded before injection of harmaline. Normalized data were averaged and presented as means ± SE. $^{*}P < 0.05$, $^{**}P < 0.01$.

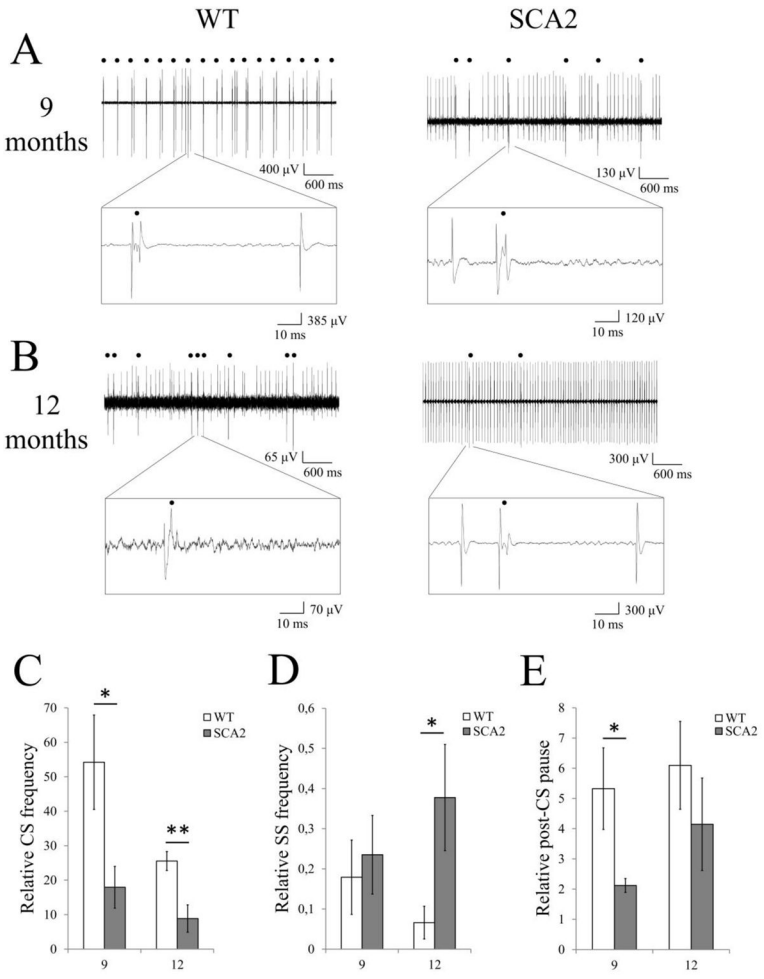

Figure 5. Changes in activity of Purkinje cells induced by injection of harmaline in 9 months old and 12 months old wild type and SCA2-58Q mice

(A, B) Examples of PC firing activity 40 min after 15 mg/kg harmaline IP injection in 9 month old (A) and 12 month old (B) wild type (left) and SCA2-58Q (right) mice. Recording traces of 5 sec in duration with enlarged 100-ms fragment are shown. Complex spikes are marked by filled circles.

(C–E) Effects of harmaline injection on PC activity pattern in 9 months old and 12 months old wild type (n = 6 and n = 6 cells; m = 6 and m = 6 mice accordingly) and SCA2-58Q mice (n = 7 and n = 5 cells; m = 7 and m = 5 mice accordingly). The CS firing frequency (*C*), SS firing frequency (*D*) and post-CS pause (*E*) for each cell were determined 40 min after injection of harmaline and normalized to the same parameters of the same cell recorded before injection of harmaline. Normalized data were averaged and presented as mean ± SE. $*P < 0.05$, $**P < 0.01$.

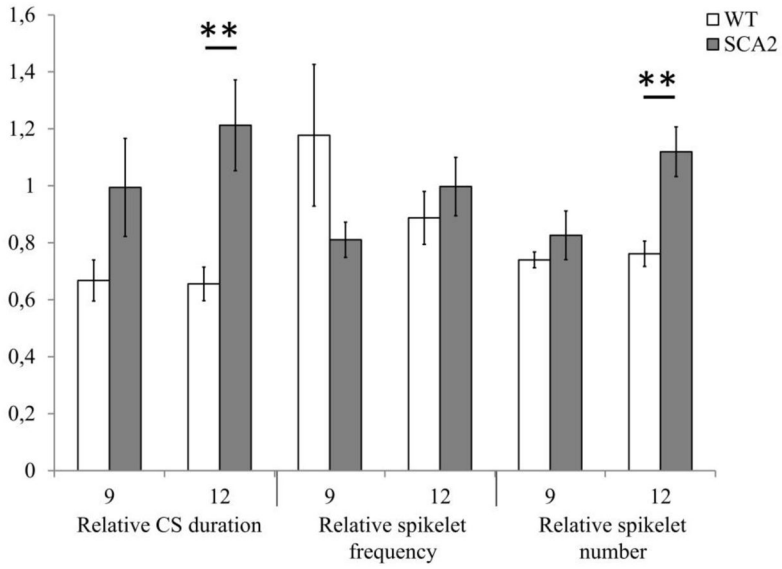

Figure 6. Effects of harmaline administration on CS shape properties for aging WT and SCA2 mice

CS duration, spikelet frequency and spikelet number for each cell were normalized to the same parameters of the same cell recorded before injection of harmaline. Analysis was performed for 9- and 12-month-old WT (n = 6 and 6 cells; m = 6 and 6 mice) and SCA2-58Q mice of the same age (n = 7 and 5 cells; m = 7 and 5 mice). The data were averaged and are presented as means ± SE. $^{**}P < 0.01$.